From vanishing interaction to superferromagnetic dimerization: Experimental determination of interaction lengths for embedded Co clusters

Arnaud Hillion, Alexandre Tamion,* Florent Tournus, Clément Albin, and Véronique Dupuis
Université de Lyon, Université Lyon 1, CNRS, Institut Lumière Matière UMR 5306, 69622 Villeurbanne, France
(Received 8 June 2016; revised manuscript received 23 January 2017; published 27 April 2017)

We report on the magnetic properties of Co clusters (around 2.5 nm diameter) embedded in different matrices (C, Au, and Cu). Firstly, we accurately determine the intrinsic magnetic properties of the particles, using highly diluted samples where no interactions are detected, and a procedure relying on the theoretical description of various magnetometry measurements, and we show how both the magnetic size and anisotropy can be impacted by the nature of the matrix. Then, by considering nanoparticle assemblies of increasing concentrations, we investigate the effects of interactions between particles. In order to account for the observed evolution of the measurements, we propose a simple model where magnetic dimers are formed for distances lower than a given interaction length (of the order of one nanometer). This superferromagnetic correlation, which can be consistently inferred for each matrix, modifies the magnetic size distribution, which has a drastic effect as soon as particles are close enough to each other.

DOI: 10.1103/PhysRevB.95.134446

I. INTRODUCTION

Magnetic nanoparticles are of great interest in a wide range of disciplines, including magnetic fluids, catalysis, biotechnology/biomedicine, magnetic resonance imaging, data storage, and environmental remediation [1–13]. Successful applications of such magnetic nanoparticles in the areas listed above are highly dependent on the stability of the particles under a range of different conditions. In particular, these nanomagnets might be used as magnetic media in future high-density magnetic storage devices with ultimate recording bits, i.e., a single nanoparticle or even a single atom [14]. Reading and writing of such a system requires to know perfectly its magnetic properties in particular its anisotropy constant. It is then crucial to be able to characterize the magnetic properties of nanoparticles, and to be able to separate the intrinsic behavior from other effects coming from interparticle interactions in an assembly.

In this paper, we present magnetic measurements of Co clusters (around 2.5-nm diameter) embedded in different matrices: carbon and two metallic matrices (Au and Cu). After a section briefly describing the sample preparation (Sec. II), we show that by using highly diluted samples, we can reach a situation where no interactions are detected. As shown in Sec. III, the intrinsic magnetic properties of the particles can then be accurately determined thanks to a "global" fitting procedure relying on the theoretical description of various magnetometry measurements [15–19]: low-temperature (hysteresis) and high-temperature (superparamagnetic) $m(H)$ loops, zero-field cooled (ZFC)/field cooled (FC) susceptibility curves, and isothermal remanent magnetization (IRM) curves. We show how both the magnetic size and magnetic anisotropy energy (MAE) can be impacted by the nature of the matrix. Then, in Sec. IV, by considering nanoparticle assemblies of increasing concentrations (still remaining in a diluted range, lower than 10% in volume), we discuss the different effects of interactions between particles on the magnetic measurements. In order to account for the observed evolution of the curves, we propose a simple model where magnetic dimers are formed for distances lower than a given interaction length. This superferromagnetic correlation, which can be consistently inferred for each matrix, thus modifies the magnetic size distribution which has a drastic effect (in particular on ZFC/FC curves) as soon as particles are close enough from each other. The deduced interaction length (of the order of one nanometer) is found to be larger for metallic matrices and could be ascribed to RKKY interactions between neighboring magnetic nanoparticles.

II. SAMPLE PREPARATION

Co clusters are preformed in the gas phase and deposited using the low-energy cluster beam deposition (LECBD) technique [20]. Briefly, clusters are produced in a laser vaporization-gas condensation source. A plasma is created by the impact of a Nd:YAG (yttrium aluminum garnet) laser beam focused on a Co rod, and thermalized by injection of a continuous flow of helium at low pressure inducing the cluster growth. Then, the clusters are cooled down in the supersonic expansion taking place at the exit nozzle of the source. A low-energy cluster beam is obtained and particles are codeposited under ultrahigh vacuum conditions (10^{-10} mbar in static pressure condition and 10^{-8} mbar during the deposition, because of the ultra pure He gas) simultaneously with the atomic beam of the matrix. Such a codeposition technique avoids any oxidation of the clusters. The samples are formed by Co nanoparticles around 2.5 nm in diameter and their diameter probability density function (PDF) closely follows a log-normal distribution. Another important feature of the LECBD technique is that the clusters arrive on the substrate (5×5 mm) in a soft-landing regime, following a random deposition scheme. As a consequence, the interparticle distance is entirely controlled by the cluster volume density [21]. This allows us to easily adjust the strength of interparticle interactions down to highly diluted samples and to study assemblies of almost isolated clusters. The *geometric* size distribution of the incident

*alexandre.tamion@univ-lyon1.fr

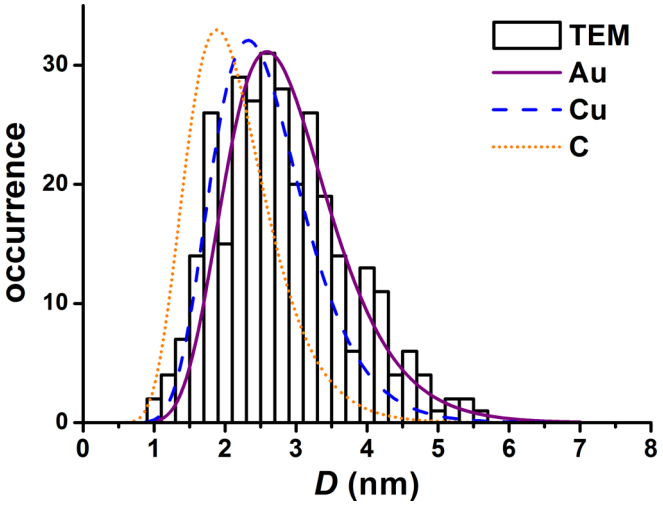

FIG. 1. Particle size distribution (PDF) of the deposited Co nanoparticles deduced from TEM observations (bars), compared to the magnetic size distribution in each matrix (Au, Cu, and C) deduced from the fits of magnetic measurements (see Sec. III). Here, the particles have been deposited on the thin amorphous carbon film of a commercial TEM grid, and subsequently capped with amorphous carbon.

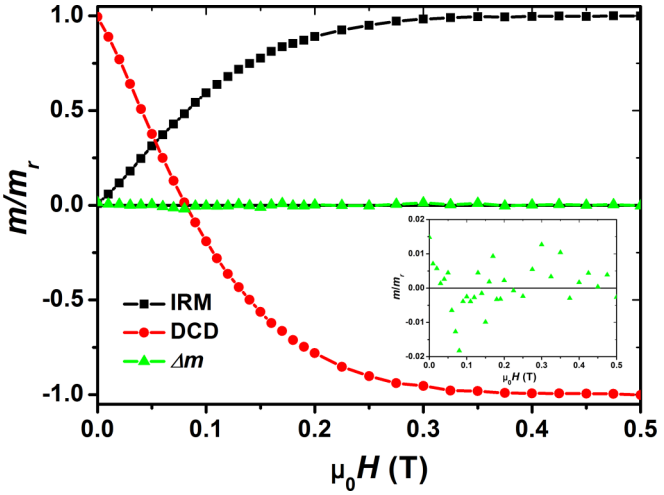

FIG. 2. IRM, DcD and Δm curves at 2 K for the sample of Co nanoparticles in a Cu matrix (0.2%). With such a dilution, there is no detectable magnetizing ($\Delta m > 0$) or demagnetizing ($\Delta m < 0$) interactions between nanomagnets. In inset, zoom on the Δm curve, which is at the background noise level.

Co clusters, as deduced from transmission electron microscopy (TEM) observations, is shown in Fig. 1, where it is compared to the *magnetic* size distribution deduced from the magnetometry measurements (see Sec. III).

All magnetic measurements have been performed in a commercial superconducting quantum interference device (SQUID) magnetometer (Quantum Design MPMS 5XL) at various temperatures. The diamagnetic response of the silicon substrate has been thoroughly characterized and all curves are corrected for this contribution. Different protocols are used to characterize the samples: $m(H)$ loops at low and room temperature, low-field susceptibility curves (ZFC/FC, with a 5-mT applied field) and isothermal remanent magnetization (IRM) together with direct-current demagnetization (DcD) curves at low temperature. These two kinds of closely related measurements, where the initial configuration is different, only probe the irreversible magnetization changes [19] and are used to characterize the nature of interactions via the parameter $\Delta m = \mathrm{DcD}(H) - [m_R - 2\mathrm{IRM}(H)]$, with m_R the remanent magnetic moment (after having saturated the sample). This parameter should be equal to zero when interparticle interactions are negligible [18,22]. An example of IRM, DcD, and the corresponding Δm curve is given in Fig. 2 for Co clusters in a Cu matrix (with a 0.2% volume concentration): in this case, there is no detectable magnetizing ($\Delta m > 0$) or demagnetizing ($\Delta m < 0$) interactions between nanomagnets.

III. INFLUENCE OF THE SURROUNDING MATRIX FOR NONINTERACTING PARTICLES

In this part, great care has been taken to minimize direct (exchange) and indirect (RKKY and dipolar) interactions between nanoparticles that prevent unambiguous determination of the Co clusters intrinsic magnetic properties. This is achieved by using low-concentration samples (<1 vol.%), which corresponds to a mean interparticle distance higher than 7-nm center to center [21] (keeping in mind that the Co nanoparticles diameter is around 2.5 nm). With these highly diluted samples, we can verify that the condition $\Delta m \approx 0$ is always valid (see Fig. 2 for the example of a Cu matrix).

The high- (300 K) and low-temperature (2 K) magnetization loops, ZFC/FC susceptibility curves, as well as the low temperature (2 K) IRM curve are shown in Fig. 3 for each matrix. The ZFC/FC curves display the characteristic behavior of an assembly of magnetic nanoparticles, namely a crossover between the low-temperature blocked regime and the superparamagnetic regime at high temperature. At first glance, the curves are modified according to the matrix used. The ZFC peak temperature ($T_{\max}$) and the coercive field at low-temperature $\mu_0 H_c$ both vary by a factor three depending on the nature of the embedding matrix (see Table I). Just focusing on these particular points, a hasty conclusion would suggest that the anisotropy constant is tripled in gold with respect to carbon. However, a more reliable analysis is possible thanks to a previously developed theoretical framework enabling a "global" fitting procedure of the entire set of magnetic measurements. Here we extend the already powerful "triple" fit approach, where ZFC/FC curves and a superparamagnetic magnetization loop are simultaneously fitted with a semianalytical model [15,21,23], and also take into account the low-temperature hysteresis loop and IRM curve which bear distinct signatures of the particles magnetic properties [17–19,24,25]. The magnetic measurements can then be reproduced with a limited number of parameters used to describe the nanomagnets (which behave as noninteracting macrospins): the magnetic size distribution (lognormal with a median diameter D_m and a dimensionless dispersion w), the anisotropy constant distribution (assumed to be gaussian with a median anisotropy constant K_1 and a standard deviation σ_{K_1}), and the biaxial anisotropy ratio K_2/K_1. The anisotropy

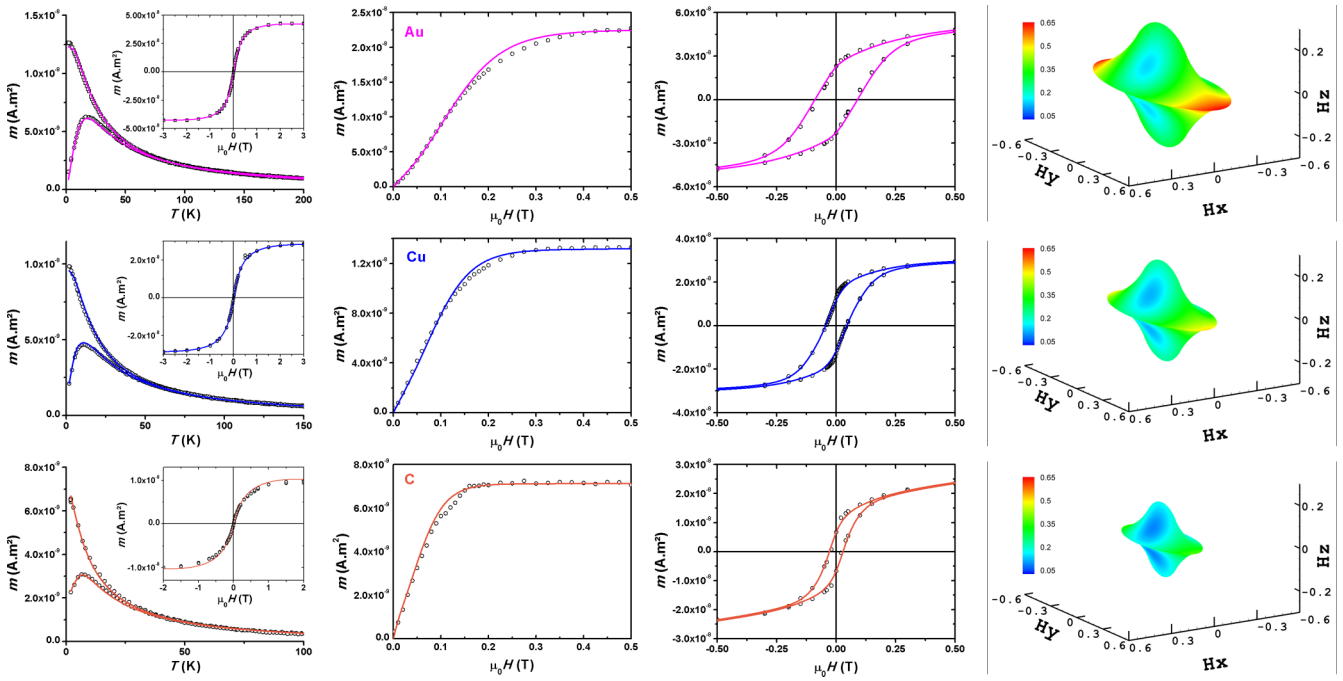

FIG. 3. Experimental and simulated ZFC/FC susceptibility curves, superparamagnetic magnetization loop (at 300 K), IRM curve and hysteresis loop at 2 K, for Co clusters embedded in different matrices: Au (0.5% vol.), Cu (0.2% vol.), and C (0.5% vol.)(from top to bottom). For each matrix, the various curves are fitted with the same set of parameters. The consideration of a second order anisotropy term K_2 (the corresponding 3D astroid is shown at the right for each matrix) and a distribution of anisotropy constant K_1 are required to reproduce all the curves.

function is expressed as [26]

$$G(\theta,\varphi) = -K_1 m_z^2 + K_2 m_y^2, \tag{1}$$

with z the easy axis, y the hard axis, and x the intermediate axis. m_z and m_y are the normalized magnetization projection on the easy z and y axis ($m_z = \mathbf{M}\cdot\mathbf{e}_z/\|\mathbf{M}\|$). The results deduced from the global fit presented in Fig. 3 for each matrix are summarized in Table I and the magnetic size distributions are compared to the geometric PDF in Fig. 1.

For the carbon matrix, one can see that the magnetic diameter is reduced by about 1 nm, which approximately corresponds to two atom-thick magnetically dead layer (i.e., with a very low magnetic signal). Such an effect of the matrix has already been reported [16,26] and it had been shown that this dead layer can disappear by using an appropriate annealing [16]. On the contrary, for the metallic matrices (Au and Cu), the magnetic PDF is found to be in good agreement with the one obtained from TEM. This result proves that there is no interdiffusion at the Co/Au, while for the Cu matrix, the incident and magnetic size seem to be slightly different.

Besides this effect of the interface on the magnetic size of the nanoparticles, we can detect a significant impact of the matrix nature on the magnetic anisotropy constant. This kind of behavior is expected since hybridization at the nanoparticle surface will depend on the atomic environment, thus modifying the electronic structure when the matrix is changed [26–30]. Note, however, that the anisotropy values remain in the same range for all the matrices.

Let us insist on the fact that T_{max} does not increase in the same proportions as the anisotropy constant K_1 (see Table I). This can be understood because the shape of ZFC/FC curves is controlled by the distribution of magnetic anisotropy energy, that is, the product of the anisotropy constant and the particle magnetic volume. Therefore a slight variation of the magnetic size distribution can significantly modify the MAE distribution and hence the value of T_{max} (position of the ZFC peak) [31]. These results emphasize that the use of T_{max} as an

TABLE I. For each sample, ZFC peak temperature (T_{max}), low-temperature coercivity ($\mu_0 H_c$), median magnetic diameter (D_m), and dispersion parameter (w) of the lognormal particle size distribution, median anisotropy constant (K_1) and standard deviation (σ_{K_1}) of the anisotropy constant distribution, and biaxial anisotropy ratio K_2/K_1 determined by a global fit of the ZFC/FC suscpetibility curves, low-temperature IRM curve, and $m(H)$ loops at 2 and 300 K. The median diameter and the dispersion parameter were found to be 2.6 nm and 0.28, respectively, by TEM.

Sample	T_{max}(K)	$\mu_0 H_c$(mT)	D_m(nm)	w	K_1(kJ/m^3)	σ_{K_1}(kJ/m^3)	K_2/K_1
Co: Au	17	85	2.8 ± 0.2	0.26 ± 0.05	190 ± 10	90 ± 10	1.3 ± 0.1
Co: Cu	12	40	2.5 ± 0.2	0.27 ± 0.05	155 ± 10	62 ± 7	1.2 ± 0.1
Co: C	6.5	25	2.1 ± 0.2	0.31 ± 0.05	115 ± 10	40 ± 5	1.2 ± 0.1

indication of the magnetic anisotropy of nanoparticles can be misleading.

The distribution of magnetic anisotropy constants K_1 (here assumed to be gaussian for simplicity) and the biaxial contribution can be explained by the additional or incomplete facets at the surface of the particles [32–34]. The relative dispersion of anisotropy constant σ_{K_1}/K_1 is nearly the same for all the matrices and is around 40%. In addition, there is no modification (within the error bars) of the ratio K_2/K_1 depending on the matrix. This study indicates that, despite all the matrix/interface effects, the magnetic anisotropy of the particles seems to be dominated by the shape and crystal structure of the particle surface, i.e., additional or incomplete facets [33,34].

These measurements at very low concentration can be used as references for studies on more concentrated nanoparticle assemblies. Now that the intrinsic (i.e., free from interparticle interaction) magnetic properties of the nanoparticles have been determined, one can experimentally investigate the effects of lowering the interparticle distance. In the next section, where we will go from a highly diluted to a diluted regime, we will thus consider the following questions: what is the required dilution to avoid interactions? What are the signatures of interactions? Is it possible to infer the intrinsic nanomagnet properties from measurements on a sample with interparticle interactions?

IV. SIGNATURE OF MAGNETIC INTERACTIONS

A major technological application envisaged for magnetic nanoparticles is magnetic recording, since the storage capacity can be greatly enhanced by the development of denser assemblies. However, this can involve strong dipole-dipole interactions between the particles, and in addition other kinds of magnetic interactions may also be met (RRKY or exchange-type interactions), depending on the nature of the media in which the particles are embedded. This will modify the magnetic properties of a sample and, for concentrated assemblies, collective behaviors can even be obtained (superspin-glass for instance [35–37]). Only dealing with magnetic dipolar interactions, the problem is already very complex due to their anisotropic and long-range nature, so that there are still unresolved questions concerning interacting assemblies of nanomagnets. Many theoretical studies (often by Monte Carlo simulations) have shown opposite effects: the relaxation time can be increased or decreased, with switching energy barriers that are raising or lowering [38–46]. Experimentally, numerous studies have been conducted to determine the influence of interactions on the magnetic properties of different nanoparticles [47–64]. In general, the studies report a shift of $T_{\max}$ towards higher temperature when the strength of the dipolar interactions is increased. The amplitude of this variation and its dependence with the concentration vary from study to study. For hysteresis loops, no definite pattern emerges, the coercive field as well as the remanence to saturation ratio m_r/m_s may increase or decrease depending on the system investigated.

In a nanoparticle sample, the interactions can be modulated by varying the distances between particles using different methods: particles randomly diluted in a nonmagnetic material (dispersion in a solvent, a polymer or an inorganic matrix) with a chosen concentration, multilayer samples of particles layers with a chosen number of repetition and spacer thickness [21,54], core-shell systems with a magnetic core surrounded by a shell of varying thickness [65,66]. In our case, with a co-deposition of preformed Co clusters in a matrix, the particles follow a random soft-landing process and the interparticle distances distribution is well known [21]. In particular, the mean nearest-neighbor (NN) distance can be directly controlled by choosing the particle volume concentration in the sample.

TABLE II. For each sample of Co particles diluted in Au, ZFC peak position ($T_{\max}$), coercivity ($\mu_0 H_c$), and remanence to saturation ratio (m_r/m_s) at low temperature (2 K), proportions of magnetic dimers and trimers deduced from the best fits. The intrinsec parameters are $D_m = 2.8$ nm and $w = 0.26$ for the lognormal size distribution and $K_1 = 190\,\mathrm{kJ\,m^{-3}}$.

Sample concentration	$T_{\max}$ (K)	$\mu_0 H_c$ (mT)	m_r/m_s	x_{dim} (%)	x_{trim} (%)
0.5%	17	85	0.38	2	0
1%	19	75	0.38	4.7	0.03
3%	28	75	0.38	15	4.5
4%	32	70	0.31	19	8

A. Results, example of the gold matrix

The study presented in the previous section allows us to extract the intrinsic properties of Co nanoparticles in very diluted samples (see Table I). In this section, focused on the gold matrix, the concentration of nanoparticles is gradually increased in order to accurately investigate the influence of interactions on the magnetic measurements. Figure 4 shows the normalized ZFC/FC, IRM/DcD, Δm, and hysteresis loop at 2 K for samples of the same Co nanoparticles embedded in a gold matrix with different concentrations (0.5, 1, 3, and 4% vol.). These concentrations may appear quite low in order to study the magnetic interactions, but let us note that for a volume concentration of 3%, the Co clusters (of 2.8-nm diameter) would be only 8 nm apart from each other (center-to-center NN distance) if they were placed on a cubic lattice. In the present case of a random 3D deposition, there is a distribution of NN distances and the average separation is then reduced drastically to 4.5 nm [21], which means down to around 2 nm edge-to-edge. One can then expect significant interactions between neighboring particles, even if the magnetic volume in the sample only represents a few percents. Since the incident particles are produced exactly in the same conditions, they must have the same intrinsic properties (size distribution and magnetic anisotropy constant), so that the obvious modifications visible on the magnetic measurements can be ascribed to interparticle interactions.

At first glance, one can see that the peak temperature $T_{\max}$ of ZFC curves increases significantly with concentration [see Fig. 4(a) and Table II)], which may be viewed as a signature of a MAE increase. Conversely, the maximum (low-T limit) of the FC curves decreases with concentration. On the

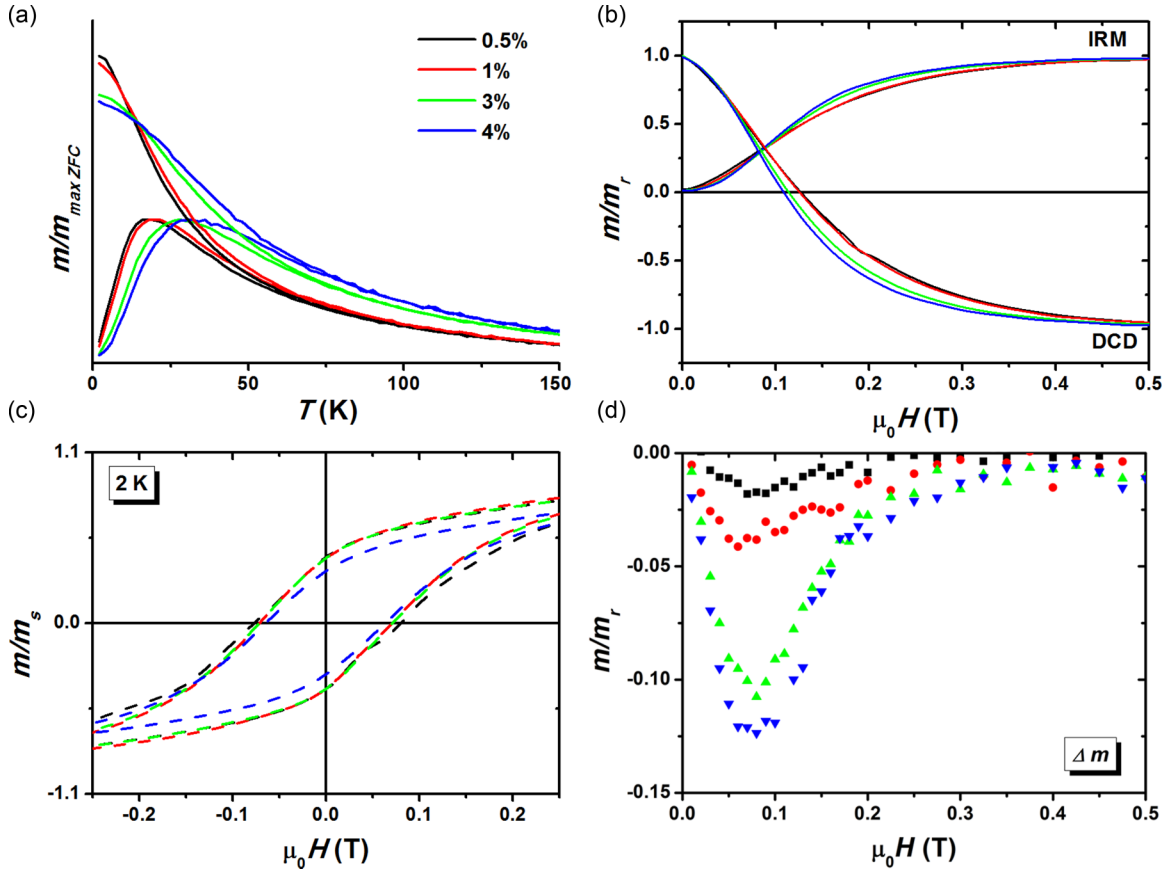

FIG. 4. (a) ZFC/FC, (b) IRM/DcD, (c) hysteresis loop, and (d) Δm curves at 2 K, for Co clusters embedded in gold with different concentrations.

other hand, the coercive field remains almost unchanged [Fig. 4(c)] and similarly the m_r/m_s ratio is constant except for the sample with the highest concentration (4% vol.), where it is equal to 0.31. Let us remind the reader that, for an assembly of randomly oriented independent macrospins with a uniaxial (or biaxial) anisotropy, the remanence to saturation ratio at zero temperature is equal to 0.5 [67]. Therefore the observation of a higher value (the ratio can only decrease with temperature) can provide a direct indication that there are interactions among the particles: this is often the case for highly concentrated nanoparticle samples, which then behave as magnetic films with inequivalent directions (easy in-plane magnetization and hard out-of-plane direction). In the case of our most concentrated sample, while we are certain to have interparticle interactions, we still observe a reduced ratio lower than 0.5, which proves that this criterion would not be sufficient to conclude that interactions are negligible in a given sample. On the contrary, the Δm curves [see Fig. 4(d)] are found to be very sensitive to interactions: while for the other magnetic measurements there are only marginal differences between the 0.5% and 1% concentrations, the Δm of the 1% sample already starts to significantly depart from zero. The negative peak in the Δm curves (which is at most around 10% of the m_r value) indicates that the interactions are rather demagnetizing and that their intensity increases with the concentration. The corresponding changes are also visible on the IRM and DcD curves, except for the two samples with the highest dilution.

Because the nanomagnets deposited in the samples are well characterized and identical in each case, we know for instance that the observed modifications are not due to a change of magnetic anisotropy constant (a hasty interpretation of the $T_{\max}$ shift could have been interpreted in such a way). In the following, we will set up a simple model able to account for the most striking changes (ZFC/FC modifications) while keeping the intrinsic nanoparticle properties unchanged. We will show that a short-range exchangelike interaction can explain in a consistent way the experimental observations on the low-field susceptibility curves. As far as the ZFC/FC curves are concerned, dipolar interactions should have a minor influence compared to this effect of magnetic dimerization.

B. Superferromagnetic dimerization

Let us focus on the susceptibility measurements: for higher concentrations, the curves cannot be reproduced with the parameters determined from the most diluted sample (0.5% vol.). Nevertheless, in the superparamagnetic regime, the curves still follow a simple $1/T$ evolution (Curie law), without any need to introduce a temperature shift often used to account for dipolar interparticle interactions (Vogel-Fulcher approach [35,37,47,68]). This shows once again that, in the considered concentration range, long-range dipolar interactions only have a minor impact on the ZFC/FC curves.

Instead of trying to take into account the magnetic dipolar interactions between the particles, we will first consider the

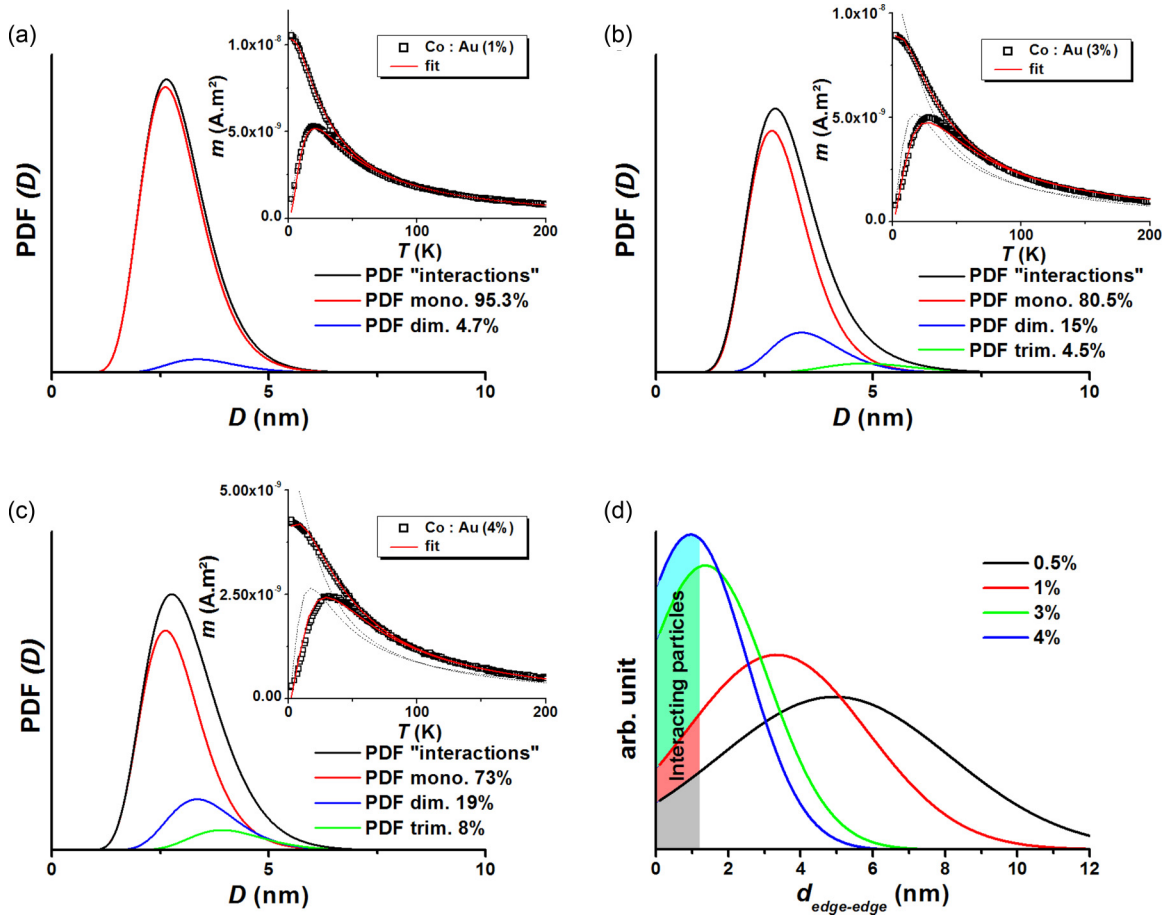

FIG. 5. (a)–(c) Resulting magnetic diameter PDF, for samples of Co particles embedded in Au (1, 3, and 4% vol. concentrations), obtained from a fit including magnetic dimers and trimers. The experimental and fitted ZFC/FC curves are shown in insert, the dashed lines correspond to the fits using monomers only. The monomer size distribution is the same as the one deduced from the sample of the lowest concentration (0.5%). (d) Statistical distribution of NN edge-to-edge distances for clusters with various concentrations (0.5, 1, 3, and 4% vol.), obtained from numerical simulations. The interaction domain is represented by a colored area which extends up to $d_{\text{edge-edge}} = \ell^*$: according to our model, Co clusters separated by less than 1.2 nm are found to be strongly coupled (superferromagnetic dimerization) in the gold matrix.

possibility of having a modification of the magnetic size distribution when the concentration is increased. This is reasonable since (i) our study is limited to samples with a quite low concentration (a few percent at most), (ii) the magnitude of the Δm peak also remains quite low (around 10% of m_r at most), and (iii) slight modifications are also observed on the superparamanetic $m(H)$ loops (see Ref. [69]), which qualitatively correspond to an increase of the magnetic size (whereas dipolar interactions in a random assembly has the opposite effect [68,70,71]).

By increasing the concentration, the average distances between the particles within the sample decreases. However, one can go beyond the consideration of only the mean NN distance, because we know that there is a statistical distribution of interparticle separations. It can then happen that two clusters are so close to each other that they cannot be considered as individual nanomagnets anymore. In an extreme case, we can even have clusters touching each other so that they form a dimer (or trimer for three clusters etc., in this case, the edge-to-edge distance is zero) [23,72]. But when two clusters remain physically separated, they can still be close enough to strongly interact from a magnetic point of view. Without considering for the moment the origin of this interaction, which may be multiple (dipolar, RKKY, exchange, etc.), one can assume that under a given NN distance called *interaction length*, neighboring particles will behave as a *magnetic dimer* (or trimer etc.). We will refer to this phenomenon with the term *superferromagnetic dimerization*: a superferromagnetic dimer is a pair of fully correlated magnetic particles, which means that their magnetic moments switch together and they behave as a single particle (macrospin) with a volume equal to the sum of their individual volume.

The theoretical distribution of NN edge-to-edge distance is shown in Fig. 5(d) for the different concentrations. When particles are almost in contact (separation lower than interatomic distances), they can physically merge and form a geometric dimer. Following this idea, numerical simulations of coalescence (geometric dimer formation for random nanoparticles in a box) have been performed on 3D sample with a cutoff distance of 1 Å for different concentrations of particles. As an example, one finds that the proportion of geometric dimers is only 2% in a sample with a 3% vol. concentration. This only marginally changes the size distribution, which then

cannot explain the significant shift observed for the ZFC peak temperature.

However, as explained above, magnetic interactions between clusters are possible without contact. These complex interactions strongly depend on the interparticle separation and can be mediated by the matrix. A first (rough) attempt to account for this phenomenon is to consider the formation of a *magnetic dimers* when the edge-to-edge distance is lower than a given interaction length ℓ^*. The value of ℓ^*, *a priori* unknown, controls the amount of magnetic multimers for each concentration (the proportion of monomers, dimers and trimers are directly related to ℓ^* and the incident particle size distribution). We then use simulations (particles randomly deposited in a box, followed by a multimer formation step when the NN distance, edge-to-edge, is lower than ℓ^*) to find a consistent value of the interaction length, able to reproduce the experimental ZFC/FC curves.

For Co clusters embedded in a gold matrix, this distance is found to be $\ell^* = 1.2 \pm 0.4$ nm (schematically indicated on Fig. 5(d). The corresponding magnetic size distributions are displayed in Fig. 5 for each dilution, with the decomposition in monomer, dimer and trimer contributions. In the 0.5% sample, this interaction length leads to the formation of approximately 2% of magnetic dimers, which does not noticeably alter the original magnetic size distribution. For the other concentrations, the proportions of dimers and trimers needed to account for the magnetic measurements are presented in Table II. These proportions can become significant: for instance, there are around 20% dimers in the sample with the highest concentration. Let us insist on the fact that ZFC low-field susceptibility curves (shape and peak position) are very sensitive to the magnetic size distribution of particles, which is why multimer formation can be detected [23] even if they are present with proportions of a few percents. This sensitivity can then help to determine quite precisely the interaction length is these nanoparticle assemblies.

It is remarkable that a single ℓ^* value is able to account for the experimental measurements of four different sets of ZFC/FC curves, as shown in Fig. 5. This gives us some confidence about the ability of our crude model to capture the essential features of the physical mechanisms involved in the magnetic interparticle interactions, at least in the range of low concentrations considered in the present study. For higher concentrations, long-range dipolar interactions may play a major role and collective effects can occur so that much more complex models are needed.

C. Other matrices and discussion

A similar study has been performed in the other matrices. Figure 6 presents the ZFC/FC and the Δm curves for Co NPs in a Cu and C matrix at different concentrations. The Δm parameter indicates that interactions (here, demagnetizing since Δm is negative) are no more negligible when the concentration is above $\simeq$1% vol., while they are not detected for the lowest concentrations of nanoparticles.

The evolution of the magnetic measurements as a function of Co clusters concentration is qualitatively the same in all the matrices. When concentration increases, the ZFC peak position $T_{\max}$ increases, the remanence to saturation ratio m_r/m_s (which is lower than 0.5) decreases, and the intensity of the Δm (negative) peak increases. Nevertheless, the behavior observed for particles in carbon is surprisingly very different from the one in copper. While the Δm peak of the most concentrated samples has a similar magnitude (around 15% of the m_r value), the $T_{\max}$ position is almost unchanged for C whereas it is nearly doubled for Cu. This suggests that, despite the fact that dipolar interactions are of comparable intensity in both samples,[1] the modifications induced on the MAE distribution are completely different. It seems that, for carbon, increasing the concentration up to a few percents has almost no impact on the ZFC/FC curves.

From what we have discussed earlier, one can think that superferromagnetic dimerization is negligible in the case of the carbon matrix. This illustrates the fact that the interaction length ℓ^* may vary from one material to another. Moreover, since one can observe significant demagnetizing interactions (magnetic dipolar interactions) without formation of magnetic dimers, this tends to prove that such a superferromagnetic dimerization must rely on other types of interactions. One can also add that dipolar interactions between neighboring particles are, in the general case, not magnetizing (it depends on the relative orientation of the clusters and of their magnetic anisotropy landscape) so that it will not produce a strong ferromagnetic correlation between NN nanomagnets.

As in the case of gold, from the fits of ZFC/FC curves, one can trace back to the interaction length ℓ^* below which two particles are strongly coupled. The simulated curves in the different matrices using magnetic dimers are presented in Fig. 7 (and Ref. [69] for Ge). We find two distinct behaviors. For nanoparticles embedded in the Cu matrix, this distance is $\ell^* = 1.3 \pm 0.2$ nm, which is very similar to the one found in the Au matrix (1.2 nm). In nonmetallic matrices (Ge and C), this distance is much smaller: 0.45 ± 0.2 nm in Ge and 0.25 ± 0.2 nm in the carbon matrix. Thus the proportion of magnetic dimers is much larger in metallic matrices. One can then think that RKKY interactions (through conduction electrons of the matrix) may be responsible for the superferromagnetic short-range interaction.

The influence of such interactions has been put into evidence in granular materials, made of magnetic particles in a metallic matrix, especially in the context of granular giant magnetoresistance (GMR) for samples with much higher concentration of magnetic element than in the present investigation [49,55,73–76]. In many studies, the role of isolated magnetic atoms diluted in the matrix has been underlined for the mediation of a sizable RKKY interaction between separated magnetic clusters, which could explain the intensity of the interparticle interactions and the effect of temperature (sample annealing). Let us note that in our case of preformed clusters deposited (soft-landing regime) in a matrix, there are no such isolated magnetic atoms in the metallic matrix, contrary to what is obtained with atomic codeposition of a nanogranular film. Beside signatures of RKKY interactions

[1] In the 4% C sample, the calculated effective dipolar field (corresponding to the mean magnetic volume and the mean nearest-neighbor distance) is equal to 88% (respectively, 53%) of that in the 3% (respectively, 5%) concentrated Cu sample.

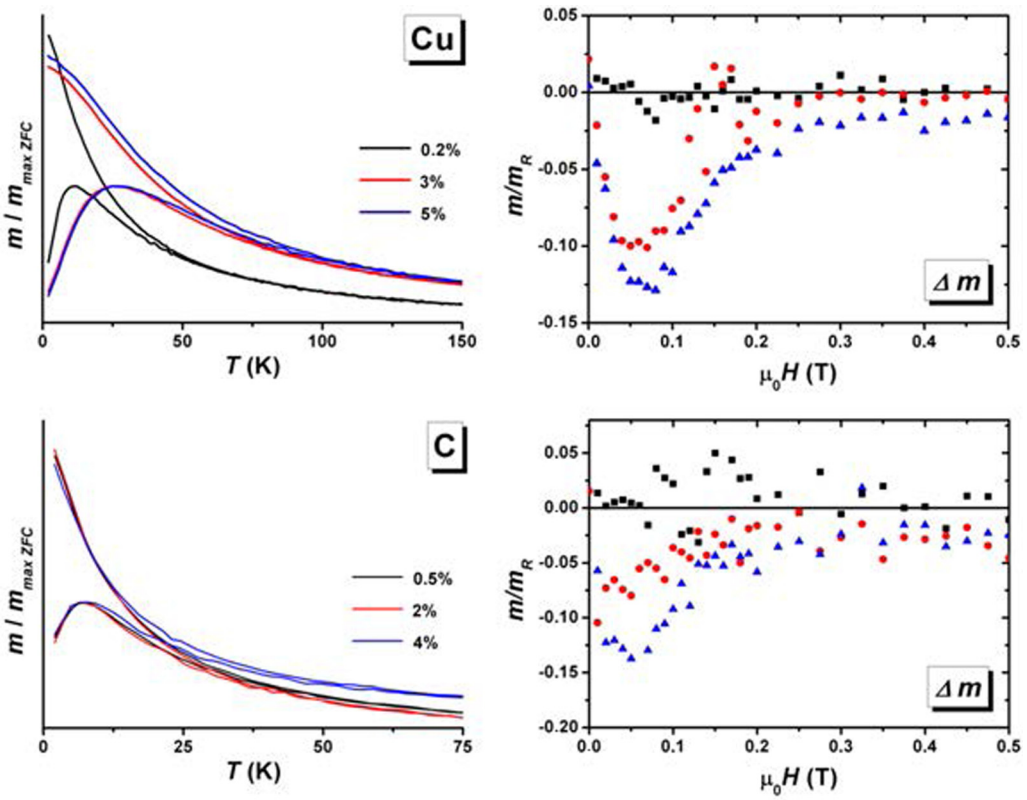

FIG. 6. ZFC/FC and Δm curves from samples of Co nanoparticles embedded in Cu and C at different concentrations. While the Δm evolution is qualitatively the same in both matrices, it is not the case of ZFC/FC curves.

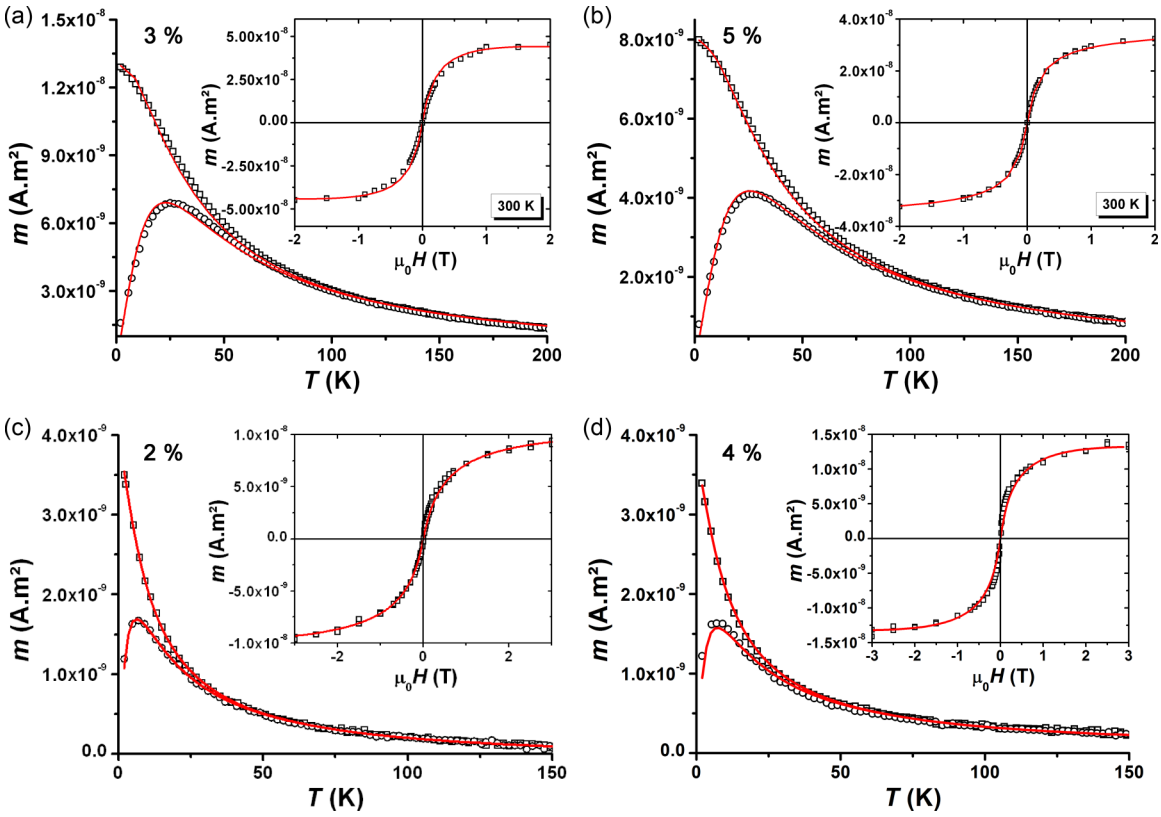

FIG. 7. Experimental (dots) ZFC/FC curves and magnetization loop at 300 K and fits (lines) using magnetic dimers and trimers for the Cu matrix [(a) and (b)] and the C matrix [(c) and (d)]. The concentration are indicated in inset.

reported for high concentrations of magnetic material (10% or higher), Herrera *et al.* [77] have recently attributed the magnetic freezing at low temperature of diluted FeAg films (Fe concentration between 0.3% and 1.5%) to RKKY interactions between small Fe clusters (of a few atoms). However, the particle size as well as the distribution of interparticle distances are not well known is this study.

It is well known that RKKY interactions display oscillations (of decreasing amplitude) with the distance, with a change of sign, i.e., corresponding either to a ferromagnetic or an antiferromagnetic interaction. Interestingly, the interaction length ℓ^* inferred from our magnetic measurements is similar to the RKKY periodicity observed for multilayers (for instance, for Co/Cu/Co, the periodicity experimentally found is around six monolayers) [78,79]. Of course, the interactions between two nanoparticles is much more difficult to describe than between two single magnetic impurities or between two magnetic layers with a metallic spacer.

There have been a few attempts of theoretical modeling for the RKKY interaction between two magnetic nanoparticles, showing that the oscillatory behavior is preserved [55,80–86]. These theoretical results may be of limited applicability, but realistic nanostructured samples remain unfortunately far from the reach of first-principles calculations [55,83,86]. Nevertheless, Qiang *et al.* [55] have performed first-principles calculations for 147-atom Co clusters in Cu and report that "the ferro- and antiferromagnetic J_{ij} for separation less than 2.5 nm are relatively large, i.e., of the order of the interatomic J_{ij} of bulk Co values and dominate over the magnetostatic interactions". However, according to some theoretical studies, over a given particle size (of the order of 100 atoms) the magnetostatic dipolar interaction should finally dominate the RKKY one [81,84].

For real nanoparticle samples, one can then expect a very complex interaction scheme, resulting from the combination of exchangelike, RKKY and dipolar interaction, with a non trivial dependance on interparticle separation and particle size (and also the particle shape and orientation, etc.). The resulting coupling will depend on the detailed structure at the nanometer scale. Anyway, according to our experimental results (interaction length in the different matrices), one can assume that RKKY interactions are the major ingredient of superferromagnetic dimerization in the metallic matrices, although exchange may also play a role (as it was considered in some theoretical studies [87,88]) and dipolar interactions can also give a ferromagnetic coupling in some configurations.

It could seem awkward to resort to RKKY interactions to account for a ferromagnetic interparticle coupling: RKKY interactions are oscillating so that one should also have neighboring particles displaying an antiferromagnetic coupling. However, even if this can happen in the sample, we have to keep in mind, first that the interaction intensity is rapidly decreasing with the distance, and second that the resulting magnetic moment for a pair of particles will be almost zero (thus undetected in the magnetic measurements!). This could explain the prominent influence of the ferromagnetically coupled particles.

It may also be unexpected to claim that ferromagnetic interparticle interactions are dominant while the Δm curve is negative, meaning that the interactions are demagnetizing. But in fact, the formation of magnetic multimers is here simply equivalent to a modification of the magnetic size distribution (a magnetic dimer behaves as a single larger particle), so that it would not result in any Δm contribution. One can also add that the modifications on the IRM/DcD curves themselves are mostly due to dipolar interactions, since they are not very sensitive to the magnetic size distribution (at zero temperature, the curves are strictly independant of the particle size [19]) and thus to the formation of magnetic dimers. On the contrary, ZFC/FC curves are highly sensitive to slight modifications of the magnetic size distribution [16,23,89] whereas dipolar interactions will shift the ZFC peak position ($T_{\max}$) only if the dipolar mean field is significant with respect to the anisotropy field. Here, this dipolar mean field remains very small in the case of ZFC/FC measurements (where the applied field is only 5 mT), while it can have a sizable impact at larger applied magnetic fields. Note that, since there is no simple theoretical description of IRM/DcD and hence of Δm for interacting nanoparticle assemblies, we could not quantitatively analyze these experimental curves for samples displaying interactions.

In the end, one can consistently explain the different magnetic measurements on Co nanoparticle assemblies, of the various concentrations considered in the present investigation, with the following features: (1) the existence of a short-range ferromagnetic interaction (superferromagnetic dimerization, certainly due to RKKY interactions) significantly modifying the ZFC/FC curves; (2) the existence of long-range dipolar interactions, having a negligible effect on susceptibility curves (and hysteresis loops) but responsible for the Δm signal.

Whatever the matrix, the long-range interactions (dipolar) are always present as it is visible in the Δm peak. On the other hand, the superferromagnetic interaction length ℓ^* (formation of magnetic dimers) depends on the matrix nature. It has been possible to infer its value in each matrix, thanks to our experimental approach where the very same Co nanoparticles are diluted in a matrix with a concentration (and thus interparticle distance distribution), which can be adjusted.

V. CONCLUSION

In summary, we have presented an accurate analysis of the magnetic size distributions and of the magnetic anisotropy constants for Co nanoparticles diluted in different matrices [Au, Cu, and C, as well as Ge (Ref. [69])]. We have first considered samples with a very low particle concentration, in order to determine the Co nanoparticles intrinsic magnetic properties. The absence of any detectable interparticle interaction has been carefully verified. We find that, in the metallic matrices, the inferred diameter distributions are consistent with the one determined by transmission electron microscopy, while a dead layer is present in the case of the C matrix. In addition, thanks to a combined fit of several magnetometry curves, the presence of a biaxial anisotropy and of a distribution of magnetic anisotropy constants has been put into evidence. Different values are found depending on the matrix, which emphasizes the role of the interface.

The modifications of the magnetic curves as a function of the nanoparticle concentration have then been discussed. For concentrations higher than typically 1% vol., interactions are unambiguously detected (through Δm measurements) and

the experimental curves can be strongly altered, although the incident Co particles still have the same intrinsic properties. Here again, the situation is different for each matrix. We finally show that, for the considered range of concentration, the ZFC/FC curves also reflect the intrisic properties of nanoparticles if the formation of magnetic dimers is taken into account: a *superferromagnetic dimerization* is supposed to occur between neighboring particles at a distance lower than the interaction length ℓ^*. This distance can be consistently inferred from measurements on a set of particle assemblies of different concentrations. The interaction length is found to be around 1.2 nm in the metallic matrices, a distance compatible with RKKY interactions, while it is much smaller in Ge and C. This phenomenon, modifying the effective magnetic size distribution when concentration is changed, has a major impact on the magnetic measurements (especially ZFC/FC curves). Our approach, where the very same Co nanoparticles are diluted in a matrix with a concentration (and thus interparticle distance distribution) that can be adjusted, provides an original and quite unique way to experimentally probe interparticle interactions (both short-range and long-range) between nanomagnets.

ACKNOWLEDGMENTS

This work has been funded through the "Agence National de la Recherche" (ANR DYSC), the "Plateforme LYonnaise de Recherche sur les Agrégats" (PLYRA), the "Centre de Magnétométrie de Lyon" (CML), the F+ 13 – 00208 application and the FWO "Pegasus Marie Curie" fellowship.

[1] M. Shliomis and V. Stepanov, J. Magn. Magn. Mater. **122**, 176 (1993).
[2] S. U. Son, Y. Jang, J. Park, H. B. Na, H. M. Park, H. J. Yun, J. Lee, and T. Hyeon, J. Am. Chem. Soc. **126**, 5026 (2004).
[3] Y. Chen, F. Yang, Y. Dai, W. Wang, and S. Chen, J. Phys. Chem. C **112**, 1645 (2008).
[4] W.-R. Lee, M. G. Kim, J.-R. Choi, J.-I. Park, S. J. Ko, S. J. Oh, and J. Cheon, J. Am. Chem. Soc. **127**, 16090 (2005).
[5] Z. Fan, M. Shelton, A. K. Singh, D. Senapati, S. A. Khan, and P. C. Ray, ACS nano **6**, 1065 (2012).
[6] A. K. Gupta and M. Gupta, Biomaterials **26**, 3995 (2005).
[7] T. A. Larson, J. Bankson, J. Aaron, and K. Sokolov, Nanotechnology **18**, 325101 (2007).
[8] A.-H. Lu, E. L. Salabas, and F. Schüth, Angewandte Chemie (International ed. in English) **46**, 1222 (2007).
[9] R. Sharma and C. J. Chen, J. Nanopart. Res. **11**, 671 (2008).
[10] C. Xu, K. Xu, H. Gu, X. Zhong, Z. Guo, R. Zheng, X. Zhang, and B. Xu, J. Am. Chem. Soc. **126**, 3392 (2004).
[11] D. L. Huber, Small (Weinheim an der Bergstrasse, Germany) **1**, 482 (2005).
[12] D. M. Newman, M. L. Wears, M. Jollie, and D. Choo, Nanotechnology **18**, 205301 (2007).
[13] S. Sun, Science **287**, 1989 (2000).
[14] P. Gambardella, S. Rusponi, M. Veronese, S. S. Dhesi, C. Grazioli, A. Dallmeyer, I. Cabria, R. Zeller, P. H. Dederichs, K. Kern, C. Carbone, and H. Brune, Science (New York, N.Y.) **300**, 1130 (2003).
[15] A. Tamion, M. Hillenkamp, F. Tournus, E. Bonet, and V. Dupuis, Appl. Phys. Lett. **95**, 062503 (2009).
[16] A. Tamion, M. Hillenkamp, A. Hillion, F. Tournus, J. Tuaillon-Combes, O. Boisron, S. Zafeiratos, and V. Dupuis, J. Appl. Phys. **110**, 063904 (2011).
[17] A. Tamion, E. Bonet, F. Tournus, C. C. Raufast, A. Hillion, O. Gaier, and V. V. Dupuis, Phys. Rev. B **85**, 134430 (2012).
[18] A. Hillion, A. Cavallin, S. Vlaic, A. Tamion, F. Tournus, G. Khadra, J. Dreiser, C. Piamonteze, F. Nolting, S. Rusponi, K. Sato, T. J. Konno, O. Proux, V. Dupuis, and H. Brune, Phys. Rev. Lett. **110**, 087207 (2013).
[19] F. Tournus, J. Magn. Magn. Mater. **375**, 194 (2015).
[20] A. Perez, V. Dupuis, J. Tuaillon-Combes, L. Bardotti, B. Prevel, E. Bernstein, P. Mélinon, L. Favre, A. Hannour, and M. Jamet, Adv. Eng. Mater. **7**, 475 (2005).
[21] F. Tournus, J. Nanopart. Res. **13**, 5211 (2011).
[22] E. P. Wohlfarth, J. Appl. Phys. **29**, 595 (1958).
[23] F. Tournus, A. Tamion, N. Blanc, A. Hillion, and V. Dupuis, J. Appl. Phys. **109**, 07B502 (2011).
[24] F. Tournus, A. Tamion, A. Hillion, and V. Dupuis, J. Magn. Magn. Mater. **419**, 1 (2016).
[25] A. Hillion, A. Tamion, F. Tournus, O. Gaier, E. Bonet, C. Albin, and V. Dupuis, Phys. Rev. B **88**, 094419 (2013).
[26] A. Tamion, C. Raufast, M. Hillenkamp, E. Bonet, J. Jouanguy, B. Canut, E. Bernstein, O. Boisron, W. Wernsdorfer, and V. Dupuis, Phys. Rev. B **81**, 144403 (2010).
[27] X. Chuanyun, Y. Jinlong, D. Kaiming, and W. Kelin, Phys. Rev. B **55**, 3677 (1997).
[28] S. Rohart, C. Raufast, L. Favre, E. Bernstein, E. Bonet, and V. Dupuis, Phys. Rev. B **74**, 104408 (2006).
[29] F. Luis, F. Bartolomé, F. Petroff, J. Bartolomé, L. M. García, C. Deranlot, H. Jaffrès, M. J. Martínez, P. Bencok, F. Wilhelm, A. Rogalev, and N. B. Brookes, Europhys. Lett. **76**, 142 (2006).
[30] J. Bartolomé, L. M. García, F. Bartolomé, F. Luis, R. López-Ruiz, F. Petroff, C. Deranlot, F. Wilhelm, A. Rogalev, P. Bencok, N. B. Brookes, L. Ruiz, and J. M. González-Calbet, Phys. Rev. B **77**, 184420 (2008).
[31] F. Tournus and A. Tamion, J. Magn. Magn. Mater. **323**, 1118 (2011).
[32] M. Jamet, W. Wernsdorfer, C. Thirion, D. Mailly, V. Dupuis, P. Mélinon, and A. Pérez, Phys. Rev. Lett. **86**, 4676 (2001).
[33] S. Oyarzun, A. Tamion, F. Tournus, V. Dupuis, and M. Hillenkamp, Sci. Rep. **5**, 14749 (2015).
[34] Y. Xie and J. A. Blackman, J. Phys.: Condens. Matter **16**, 3163 (2004).
[35] J. Dormann, D. Fiorani, and E. Tronc, J. Magn. Magn. Mater. **202**, 251 (1999).
[36] J. A. De Toro, S. S. Lee, D. Salazar, J. L. Cheong, P. S. Normile, P. Muñiz, J. M. Riveiro, M. Hillenkamp, F. Tournus, A. Tamion, and P. Nordblad, Appl. Phys. Lett. **102**, 183104 (2013).
[37] S. A. Majetich and M. Sachan, J. Phys. D: Appl. Phys. **39**, R407 (2006).

[38] M. Azeggagh and H. Kachkachi, Phys. Rev. B **75**, 174410 (2007).

[39] R. Malik, S. Lamba, R. K. Kotnala, and S. Annapoorni, Eur. Phys. J. B **74**, 75 (2010).

[40] M. Ulrich, J. García-Otero, J. Rivas, and A. Bunde, Phys. Rev. B **67**, 024416 (2003).

[41] D. Kechrakos, K. Trohidou, and M. Vasilakaki, J. Magn. Magn. Mater. **316**, e291 (2007).

[42] W. Figueiredo and W. Schwarzacher, Phys. Rev. B **77**, 104419 (2008).

[43] V. Russier, J. Appl. Phys. **105**, 073915 (2009).

[44] R. P. Tan, J. S. Lee, J. U. Cho, S. J. Noh, D. K. Kim, and Y. K. Kim, J. Phys. D **43**, 165002 (2010).

[45] P.-M. Déjardin, J. Appl. Phys. **110**, 113921 (2011).

[46] D. Brinis, A. Laggoun, D. Ledue, and R. Patte, J. Appl. Phys. **115**, 173906 (2014).

[47] S. H. Masunaga, R. F. Jardim, R. S. Freitas, and J. Rivas, Appl. Phys. Lett. **98**, 013110 (2011).

[48] J. De Toro, J. González, P. Normile, P. Muñiz, J. Andrés, R. López Antón, J. Canales-Vázquez, and J. Riveiro, Phys. Rev. B **85**, 054429 (2012).

[49] J. A. De Toro, J. P. Andrés, J. A. González, J. P. Goff, A. J. Barbero, and J. M. Riveiro, Phys. Rev. B **70**, 224412 (2004).

[50] J. Chen, A. Dong, J. Cai, X. Ye, Y. Kang, J. M. Kikkawa, and C. B. Murray, Nano Lett. **10**, 5103 (2010).

[51] S. K. Mishra and V. Subrahmanyam, Phys. Rev. B **84**, 024429 (2011).

[52] P. Cregg, K. Murphy, A. Mardinoglu, and A. Prina-Mello, J. Magn. Magn. Mater. **322**, 2087 (2010).

[53] M. del Muro, X. Batlle, and A. Labarta, J. Magn. Magn. Mater. **221**, 26 (2000).

[54] F. Luis, F. Petroff, J. M. Torres, L. M. García, J. Bartolomé, J. Carrey, and A. Vaurès, Phys. Rev. Lett. **88**, 217205 (2002).

[55] Y. Qiang, R. F. Sabiryanov, S. S. Jaswal, Y. Liu, H. Haberland, and D. J. Sellmyer, Phys. Rev. B. **66**, 064404 (2002).

[56] X. Zhang, G. Wen, G. Xiao, and S. Sun, J. Magn. Magn. Mater. **261**, 21 (2003).

[57] P. Poddar, T. Telem-Shafir, T. Fried, and G. Markovich, Phys. Rev. B **66**, 060403(R) (2002).

[58] D. Serantes, D. Baldomir, M. Pereiro, C. E. Hoppe, F. Rivadulla, and J. Rivas, Phys. Rev. B **82**, 134433 (2010).

[59] J. M. Vargas, W. C. Nunes, L. M. Socolovsky, M. Knobel, and D. Zanchet, Phys. Rev. B **72**, 184428 (2005).

[60] G. F. Goya, T. S. Berquó, F. C. Fonseca, and M. P. Morales, J. Appl. Phys. **94**, 3520 (2003).

[61] M. Georgescu, M. Klokkenburg, B. Erné, P. Liljeroth, D. Vanmaekelbergh, and P. Zeijlmans van Emmichoven, Phys. Rev. B **73**, 184415 (2006).

[62] C. J. Bae, S. Angappane, J.-G. Park, Y. Lee, J. Lee, K. An, and T. Hyeon, Appl. Phys. Lett. **91**, 102502 (2007).

[63] V. B. Barbeta, R. F. Jardim, P. K. Kiyohara, F. B. Effenberger, and L. M. Rossi, J. Appl. Phys. **107**, 073913 (2010).

[64] M. Georgescu, J. Viota, M. Klokkenburg, B. Erné, D. Vanmaekelbergh, and P. Zeijlmans van Emmichoven, Phys. Rev. B **77**, 024423 (2008).

[65] J. A. De Toro, P. S. Normile, S. S. Lee, D. Salazar, J. L. Cheong, P. Muñiz, J. M. Riveiro, M. Hillenkamp, F. Tournus, A. Tamion, and P. Nordblad, J. Phys. Chem. C **117**, 10213 (2013).

[66] H. T. Yang, D. Hasegawa, M. Takahashi, and T. Ogawa, Appl. Phys. Lett. **94**, 013103 (2009).

[67] E. C. Stoner and E. P. Wohlfarth, Philos. Trans. R. Soc., A **240**, 599 (1948).

[68] P. Allia, M. Coisson, P. Tiberto, F. Vinai, M. Knobel, M. A. Novak, and W. C. Nunes, Phys. Rev. B **64**, 144420 (2001).

[69] See Supplemental Material at http://link.aps.org/supplemental/10.1103/PhysRevB.95.134446 for ZFC/FC curves and magnetization loop at 300 K of Co particles in Ge matrix.

[70] Z. Mao, D. Chen, and Z. He, J. Magn. Magn. Mater. **320**, 2335 (2008).

[71] J. Al Saei, M. El-Hilo, and R. W. Chantrell, J. Appl. Phys. **110**, 023902 (2011).

[72] F. Tournus, Phys. Rev. E **84**, 011612 (2011).

[73] J. Alonso, M. L. Fdez-Gubieda, A. Svalov, C. Meneghini, and I. Orue, J. Alloys Comp. **536S**, S271 (2012).

[74] J. Du, B. Zhang, R. K. Zheng, and X. X. Zhang, Phys. Rev. B. **75**, 014415 (2007).

[75] M. Hillenkamp, G. Di Domenicantonio, and C. Félix, Phys. Rev. B. **77**, 014422 (2008).

[76] A. López, F. J. Lázaro, M. Artigas, and A. Larrea, Phys. Rev. B. **66**, 174413 (2002).

[77] W. T. Herrera, Y. T. Xing, S. M. Ramos, P. Munayco, M. B. Fontes, E. M. Baggio-Saitovitch, and F. J. Litterst, Phys. Rev. B. **84**, 014430 (2011).

[78] P. Bruno and C. Chappert, in *Magnetism and Structure in Systems of Reduced Dimension*, edited by R. F. C. Farrow *et al.* (Plenum Press, New York, 1993), p. 389.

[79] S. S. P. Parkin, R. Bhadra, and K. P. Roche, Phys. Rev. Lett. **66**, 2152 (1991).

[80] G. M. Genkin and M. V. Sapozhnikov, Appl. Phys. Lett. **64**, 794 (1994).

[81] D. Altbir, J. d'Albuquerque e Castro, and P. Vargas, Phys. Rev. B **54**, R6823 (1996).

[82] P. Vargas and D. Altbir, J. Magn. Magn. Mater. **167**, 161 (1997).

[83] R. Skomski, Europhys. Lett. **48**, 455 (1999).

[84] R. Skomski, R. F. Sabiryanov, and S. S. Jaswal, J. Appl. Phys. **87**, 5890 (2000).

[85] C.-H. Chang and T.-M. Hong, Chin. J. Phys. **47**, 703 (2009).

[86] P. A. Ignatiev, N. N. Negulyaev, A. S. Smirnov, L. Niebergall, A. M. Saletsky, and V. S. Stepanyuk, Phys. Rev. B **80**, 165408 (2009).

[87] M. El-Hilo, K. O'Grady, and R. W. Chantrell, J. Appl. Phys. **76**, 6811 (1994).

[88] D. Kechrakos and K. N. Trohidou, J. Magn. Magn. Mater. **262**, 107 (2003).

[89] A. Tamion, M. Hillenkamp, F. Tournus, E. Bonet, and V. Dupuis, Appl. Phys. Lett. **100**, 136102 (2012).